Metal-slotted hybrid optical waveguides for PCB-compatible optical interconnection

Jin Tae Kim,[1,2] Jung Jin Ju,[1] and Suntak Park[1,*]

[1]*Electronics and Telecommunications Research Institute (ETRI), Daejeon 305-700, South Korea*
[2]*jintae@etri.re.kr*
[*]*spark@etri.re.kr*

Abstract: For development of electro-optical printed circuit board (PCB) systems, PCB-compatible metal-slotted hybrid optical waveguide was proposed and its optical characteristics are investigated at a wavelength of 1.31 μm. To confine light in a metallic multilayered structure, a metal film with a wide trench is inserted at the center of a dielectric medium that is sandwiched between metal films of infinite width. A circularly symmetric spot of the guided mode was measured at the center of the metal-slotted optical waveguide, which is a good agreement with the theoretical prediction by using the finite-element method. The measured propagation loss is about 1.5 dB/cm. Successful transmission of 2.5 Gbps optical signal without any distortion of the eye diagram confirms that the proposed hybrid optical waveguide holds a potential transmission line for the PCB-compatible optical interconnection.

OCIS codes: (230.7370) Waveguides; (200.4650) Optical interconnects; (130.3120) Integrated optics devices.

References and links

1. A. V. Krishnamoorthy and D. A. B. Miller, "Scaling optoelectronic-VLSI circuits into the 21st century: a technology roadmap," IEEE J. Sel. Top. Quantum Electron. **2**(1), 55–76 (1996).
2. A. F. J. Levi, "Optical interconnections in systems," Proc. IEEE **88**(6), 750–757 (2000).
3. D. A. B. Miller, "Rationale and challenges for optical interconnects to electronic chips," Proc. IEEE **88**(6), 728–749 (2000).
4. K. H. Hahn, "POLO-parallel optical links for gigabyte data communications," in Proc. 8th Annu. Meeting LEOS, San Francisco, CA, 228–229 (1995).
5. Y. S. Liu, R. J. Wojnarowski, W. A. Hennessy, J. P. Bristow, and A. Yue Liu, Peczalski, J. Rowlette, A. Plotts, J. Stack, M. Kadar-Kallen, J. Yardley, L. Eldada, R. M. Osgood, R. Scarmozzino, S. H. Lee, V. Ozgus, and S. Patra, "Polymer optical interconnect technology (POINT)-optoelectronic packaging and interconnect for board and backplane applications," in Proc. 46th Electron. Compon. Technol. Conf., Orlando, FL, 308–315 (1996).
6. L. J. Norton, F. Carney, N. Choi, C. K. Y. Chun, R. K. Denton, Jr., D. Diaz, J. Knapp, M. Meyering, C. Ngo, S. Planer, G. Raslun, E. Reyes, J. Sauvageau, D. B. Schwartz, S. G. Shook, J. Yoder, and Y. Wen, "OPTOBUS^{TM} I: A production parallel fiber optical interconnect," in Proc. 47th Electron. Compon. Technol. Conf., San Jose, CA, 204–209 (1997).
7. H. Karstensen, L. Melchior, V. Plickert, K. Drogemuller, J. Blank, T. Wipiejewski, H.-D. Wolf, J. Wieland, G. Jeiter, R. Dal'Ara, and M. Blaser, "Parallel optical link (PAROLI) for multichannel gigabit rate interconnections," in Proc. 48th Electron. Compon. Technol. Conf., Seattle, WA, 747–754 (1998).
8. M. Usui, N. Sato, A. Ohki, N. Matsuura, N. Tanaka, K. Enbutsu, M. Amano, M. Hikita, T. Kagawa, K. Katsura, and Y. Ando, "ParaBIT-1: 60-Gb/s-throughput parallel optical interconnect module," in Proc. 50th Electron. Compon. Technol. Conf., LasVegas, NV, 1252–1258 (2000).
9. D. Krabe, F. Ebling, N. Arndt-Staufenbiel, G. Lang, and W. Scheel, "New technology for electrical/optical systems on module and board level: The EOCB approach," in Proc. 50th Electron. Compon. Technol. Conf., Las Vegas, NV, 970–974 (2000).
10. K. Schmieder and K.-J. Wolter, "Electro-optical printed circuit board (EOPCB)," in Proc. 50th Electron. Compon. Technol. Conf., Las Vegas, NV, 749–753 (2000).
11. R. N. Simons, Coplanar Waveguide Circuits, Components, and Systems (Wiley Interscience, 2001).
12. FIMMWAVE. ver. 5.0, a vectorial waveguide solver. Photon Design, 2006.
13. E. D. Palik, *Handbook of Optical Constants of Solids* (Academic, 1985).
14. D. Sarid, "Long-range surface-plasma waves on very thin metal films," Phys. Rev. Lett. **47**(26), 1927–1930 (1981).
15. J. T. Kim, J. J. Ju, S. Park, M. S. Kim, S. K. Park, and M.-H. Lee, "Chip-to-chip optical interconnect using gold long-range surface plasmon polariton waveguides," Opt. Express **16**(17), 13133–13138 (2008).

#164850 - $15.00 USD Received 16 Mar 2012; revised 9 Apr 2012; accepted 11 Apr 2012; published 20 Apr 2012

16. J. T. Kim, J. J. Ju, S. Park, S. K. Park, M.-S. Kim, J.-M. Lee, J.-S. Choe, M.-H. Lee, and S.-Y. Shin, "Silver stripe optical waveguide for chip-to-chip optical interconnection," IEEE Photon. Technol. Lett. **21**(13), 902–904 (2009).
17. E. Griese, "A high-performance hybrid electrical-optical interconnection technology for high-speed electronic systems," IEEE Trans. Adv. Packag. **24**(3), 375–383 (2001).
18. Y. Ishii, S. Koike, Y. Arai, and Y. Ando, "SMT-compatible large-tolerance "OptoBump" interface for interchip optical interconnections," IEEE Trans. Adv. Packag. **26**(2), 122–127 (2003).
19. A. L. Glebov, D. Bhusari, P. Kohl, M. S. Bakir, J. D. Meindl, and M. G. Lee, "Flexible pillars for displacement compensation in optical chip assembly," IEEE Photon. Technol. Lett. **18**(8), 974–976 (2006).

1. Introduction

In order to meet the ever-increasing demand for higher clock speed and density of input/outputs (I/Os) in interconnection, optical interconnection has been considered as a promising solution due to its excellent properties such as low loss signal transmission, high bandwidth, and immunity for electromagnetic interference (EMI) [1–3]. Both chip-to-chip and board-to-board optical interconnects are major area of research in optoelectronics to improve the data rate and bandwidth of signal transmission between electronic devices. Numerous optical interconnection schematics have been demonstrated [4–8]. Architectural concepts of electro-optical printed circuit board (EOPCB) and electrical optical circuit board (EOCB) have been exhibited their ability to transmit several gigabyte optical signals over standard distances by [9, 10].

Optical waveguides have been played a key role in development of the EOPCB systems. However, the fabrication process for forming the thick multimode waveguide cores requires costly deep etching or imprinting process, which are not compatible with the PCB manufacturing process. On the other hand, the optical waveguides in PCB layers have been used only for an optical signal guiding medium to date. In PCBs, there are metallic electrical circuits for electrical interconnection. Their structures are so called microstrip or strip-line [11]. If the optical waveguides embedded in PCB layers are compatible with such Cu-based electric circuit structures, the embedded optical waveguides serve as a multifunctional interconnection medium providing simultaneous optical and electrical interconnection. In addition, cost-effective fabrication of EOPCB system may be achievable because the conventional PCB fabrication process can be applied. Therefore, the investigation on an electric-circuit-compatible novel optical waveguide is highly required to improve the development of the EOPCB systems further.

To satisfy the demand, here, we proposed a metal-slotted hybrid optical waveguide and investigated its optical characteristics theoretically and experimentally. To confine light in conventional PCB layers, a thin metal film with a trench is embedded in a dielectric slab, and then they are sandwiched between two conductors that serve as a ground plate or electric signal transmission line in a PCB. A theoretical investigation on the characteristics of the guided mode was performed by using the finite element method. The optical characteristics of the fabricated metal-slotted hybrid optical waveguide are in a good agreement with the theoretical investigation. 2.5 Gbps high speed optical signal transmission via the proposed hybrid optical waveguide was successively performed without any distortion of the eye diagram.

2. Architectural concept and theoretical analysis

Figure 1 exhibits the proposed metal based hybrid optical waveguide structure. It consists of three Cu films. A metal-slot with a separation gap of w is embedded in a dielectric medium that is sandwiched between metal films of infinite width. The thickness of the dielectric medium (t_d) is the same to the metal-slot width (w). Thus, a square dielectric waveguide structure is formed based on metal slot. The thickness of the three metal layers is t_m. The waveguide structure proposed here is similar to the conventional coplanar waveguides that consisted of planar strip lines on a flat surface separated from a pair of ground planes [11]. The electric signal transmits via the center-metal and the optical signal transmits via the hybrid optical waveguide that is defined by metal slot and electric ground planes. Therefore,

#164850 - $15.00 USD Received 16 Mar 2012; revised 9 Apr 2012; accepted 11 Apr 2012; published 20 Apr 2012

on-board integration of the conventional PCB-compatible optical waveguides can be exploited.

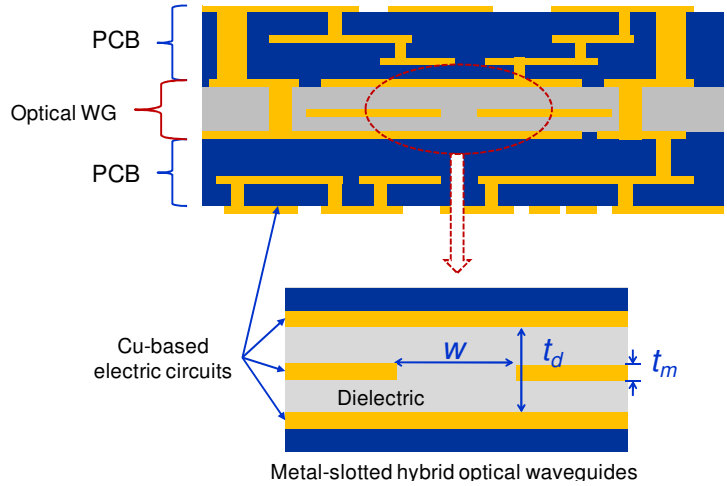

Fig. 1. Architectural concept of a metal-slotted hybrid optical waveguides. The proposed waveguide is based on metallic circuit structures in a printed circuit board (PCB) and is embedded in the conventional PCB layers.

The guided modes of the proposed hybrid coplanar optical waveguide are derived by the finite element method (FEM), using a commercial package FIMMWAVE of Photon Design [12]. The complex refractive index of Cu at the wavelength of 1.3 μm is 0.51179 + 7.01500*i* [13]. The refractive index of the dielectric material is 1.45.

If the metal-slot is not present at the center of the dielectric, the waveguide structure is considered as a slab waveguide with a metal cladding. The guided modes are confined in the vertical direction but not confined in the lateral direction because of infinite dielectric core width. The lateral confinement of mode is possible by inserting a metal film with a slot at the center of the dielectric slab.

Figure 2 shows the calculated *E*-field distribution of the guided modes supported by the proposed hybrid optical waveguide. The field profiles of each guided modes along the *x*- and *y*-axis are also exhibited. The profiles cross the center of the square dielectric medium. The guided modes are derived at a wavelength of 1.31 μm. Figure 2(a) and 2(b) represent E_x- and E_y-field distribution of the quasi-transverse-electric (TE) and transverse-magnetic (TM) modes, respectively, when w = 15 μm and t_d = 15 μm. For comparison, the field distribution of the hybrid optical waveguide with a large square dielectric core (w = 70 μm and t_d = 70 μm) are exhibited in Fig. 2 (c) and 2(d). The thickness of the metal film is 2 μm.

For the both TE- and TM-polarization, the guided modes are confined in the vertical and lateral directions by the hybrid Cu metal structures. The guided modes are like a combination of a dielectric mode and a surface plasmon polariton (SPP) mode. SPP mode is electromagnetic surface waves propagating along an interface between a dielectric and a metal [14]. For the TE-polarization, the SPP mode can be excited at the interface between the dielectric and the sidewall of the slot (two sidewalls of the center metal films). For TM-polarization, SPP modes are excited at both metal-dielectric interfaces of the upper and lower Cu metal of infinite width. The SPP is related to the damping oscillation of free electrons in metal so that the TE- and TM-polarization have an attenuation coefficient. The amplitude of the SPP mode in the TM-polarization is comparatively higher than that of the TE-polarization, as shown in Fig. 2(a) and 2(b). Thus, it is expected that the propagation loss of the TM-polarization is to be higher than that of the TE-polarization. On the other hand, the field intensity at the metal-dielectric interface of the upper and lower metal film decreases as the

#164850 - $15.00 USD Received 16 Mar 2012; revised 9 Apr 2012; accepted 11 Apr 2012; published 20 Apr 2012

waveguide size increase. This is clearly shown at the E_y-field profiles of Fig. 2(c) and 2(d) in the vertical direction. Therefore, it is also expected that the propagation loss of the hybrid optical waveguide decreases as the size of the square dielectric core increases.

The confinement of the guided mode by means of the metal slot becomes poor when the thickness of the dielectric medium and the metal-slot width increase. It is because light confinement by the metal slot is less tight. Compared to the thickness of the dielectric medium (70 μm), that of the metal slot (2 μm) is very thin. Thus, a region where is free from the metal slot is generated in the top and bottom sides in the square dielectric core. As a result, the lateral size of the guided mode in this region increases, as shown in Fig. 2(c) and 2(d). If additional metal slots are inserted above and below the metal slot, more tight confinement of the guided mode is possible with the cost of slightly increased propagation loss. The channel crosstalk is not issue because the lateral distance between the waveguide channels is larger than 250 μm, which is large enough to suppress the mode coupling between the waveguide channels.

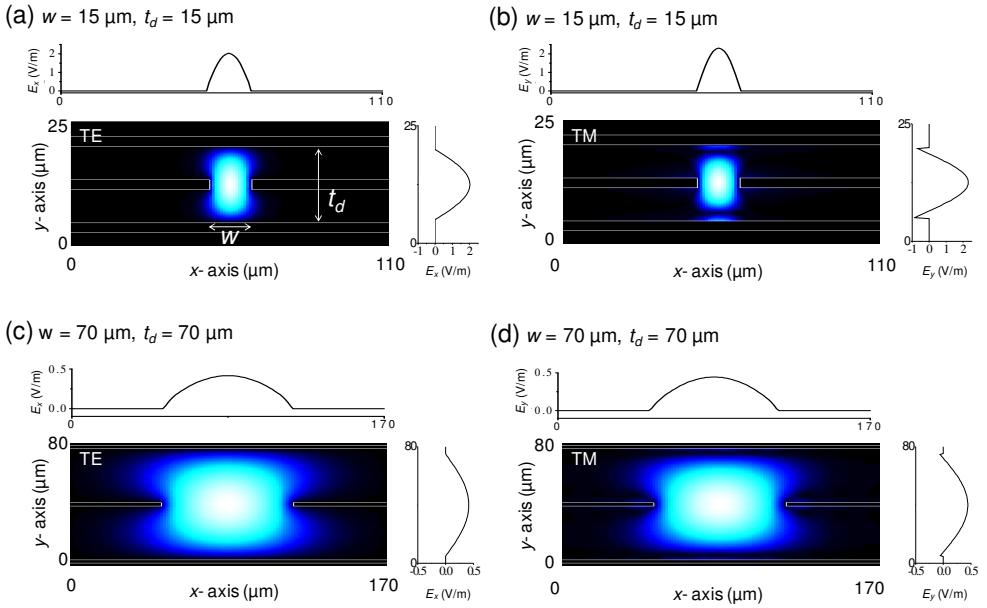

Fig. 2. Calculated *E*-field distribution of the guided modes. (a) and (c) are the quasi-TE mode. (b) and (d) are quasi-TM modes. The field profiles along the *x*- and *y*-axis are also exhibited.

Figure 3 exhibits the calculated propagation loss of the proposed metal-slotted hybrid optical waveguide depending on the metal-slot width w and the metal film thickness t_m. The metal slot-width and the dielectric thickness are the same ($w = t_d$). As the metal-slot width decrease (the dielectric thickness decreases too), the propagation loss of the guided hybrid mode increases gradually. It increases noticeably if the metal-slot width is smaller than 30 μm. For the waveguide having a wide metal-slot and a thick dielectric, the amplitude of the lossy SPP mode at the metal-dielectric interface is comparatively low. This is shown in the field profiles of Fig. 2(c) and 2(d). The guided modes of the both TE- and TM polarization propagate along the waveguide with low attenuation. In the contrast, the waveguides with a small metal-slot width and a thin dielectric medium confine the field of the guided mode tightly in the dielectric region. The field intensity at the metal-dielectric interface is comparatively high. This is clearly shown in Fig. 2(a) and 2(b). The affect of the lossy SPP mode on the propagation characteristics is dominant for the both TE- and TM-polarizations. As a result, the propagation loss of the guided modes increases as the metal-slot width decreases. The propagation losses of the TE-polarization modes are slightly lower than those

#164850 - $15.00 USD Received 16 Mar 2012; revised 9 Apr 2012; accepted 11 Apr 2012; published 20 Apr 2012

of TM-polarization modes. This is due to the fact that the field profiles of the TE-polarization are slightly associated with the lossy SPP mode at the metal-dielectric interfaces. If the metal slot width is larger than 40 μm, the calculated propagation loss of the TE-polarization could be lower than 1 dB/cm. The propagation loss o the hybrid optical waveguide is highly dependent on the metal film thickness (t_m). As the film thickness increase the field is confined more tightly to the metal film. Thus, losses due to metal increases and the propagation loss increases as the metal film thickness increases.

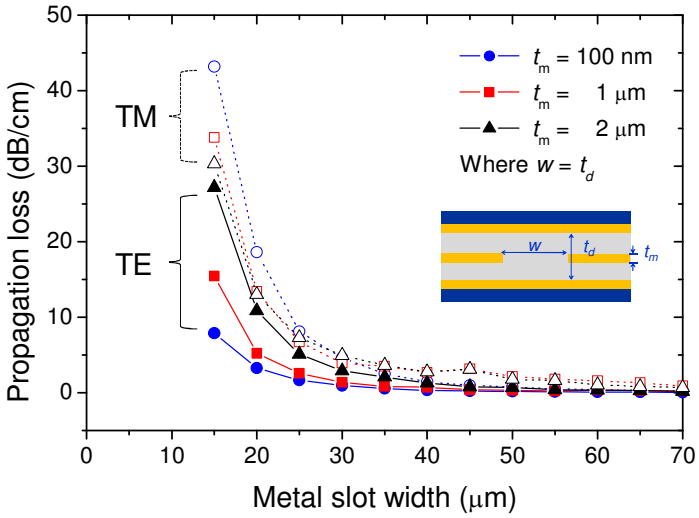

Fig. 3. Calculated propagation loss of the proposed metal-slotted hybrid optical waveguides depending on the metal slot width and metal film thickness. The metal-slot width is the same to the dielectric thickness ($w = t_d$). The inset shows the waveguide structure.

3. Experiment and discussions

In order to confirm the theoretical prediction, we fabricated the proposed metal-slotted hybrid optical waveguide. First, base dielectric material was formed to be 10 μm by spin-coating and UV curing. Then, 200 nm-thick Cu thin film was evaporated thermally on the base polymer material. The lower-cladding layer was formed to be 50 μm by spin-coating and UV curing. Consequently, photo-resist is spin coated on the lower-cladding layer and 200 nm-thick Cu was evaporated thermally again on the pre-patterned thick photo-resist. After removal of the PR, 100 μm-wide slotted Cu film is formed on the lower-cladding layer. 50 μm-thick upper-cladding layer was formed on the slotted Cu film by spin-coating and UV curing. Finally, 200 nm-thick Cu thin film was evaporated thermally. The metal-slot width and the dielectric thickness of the hybrid optical waveguide are 100 μm and 100 μm, respectively.

For the dielectric medium, we used a commercial UV-curable polymer, Exguide ZPU series from ChemOptics (www.chemoptics.co.kr). This optical polymer material provides low propagation loss of less than 0.1 dB/cm and low birefringence (n_{TE} - n_{TM}) of 0.001 ± 0.0003 at a wavelength of 1.31 μm.

To investigate the characteristics of the fabricated metal-slotted optical waveguide, the light from a source is launched at the input facet of the fabricated waveguides by using a single-mode (SMF) and multi-mode fiber (MMF). The infrared images of the guided mode were measured by a charge-coupled device (CCD). After measuring the infrared images, the output light were collected by a SMF or MMF, and the transmitted powers were measured with an optical power meter to evaluate insertion loss.

Figure 4 exhibits the characteristics of the fabricated metal-slotted hybrid optical waveguide. Figure 4(a) shows the infrared image of the observed far-field guided mode measured by using a charge-coupled device (CCD). The guided mode is excited by the SMF.

#164850 - $15.00 USD Received 16 Mar 2012; revised 9 Apr 2012; accepted 11 Apr 2012; published 20 Apr 2012

White dot lines guide the Cu thin film consisting of the proposed hybrid optical waveguide. A circularly symmetric spot is measured at the center of the metal-slotted waveguide. The two-dimensional mode confinement results in the formation of circular light spot. The slight position shift of the input fiber in the vertical and lateral direction generates diminished the intensity of the light spot. However, the similar circularly symmetric spots are observed if the input fiber moves 500 μm in the left and right direction, where another waveguide is present.

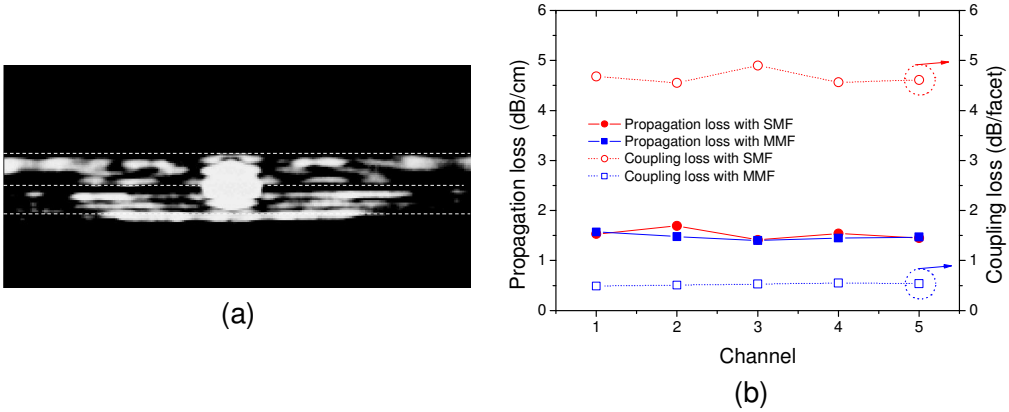

Fig. 4. Characteristics of the metal-slotted hybrid optical waveguide. (a) Infrared image of the observed far-field guided mode: white dot lines guide the Cu thin film consisting of the proposed hybrid optical waveguide. (b) Measured propagation and coupling losses.

Figure 4(b) shows the measured propagation loss for five different waveguide channels by using a SMF and a MMF. The propagation loss is 1.5 dB/cm in average. The dependence of the propagation loss on the size of the butt-coupled fiber core is not measured. However, the coupling loss of the waveguide is highly dependent on the size of the fiber core. For a SMF, the mode field diameter (MFD) is about 9.2 μm at 1.31 μm wavelength. The MFDs of the fabricated hybrid optical waveguide in the horizontal and the vertical directions are about 75 μm and 70 μm, respectively. Therefore, the MFD mismatch between the SMF and the hybrid optical waveguide is large. The coupling loss with a SMF is high as 4.5 dB, as shown in Fig. 4(b). On the contrary, the MFD mismatch between the MMF and the hybrid optical waveguide is low, because the MFD of the MMF is 62.5 μm. The averaged coupling loss of the hybrid optical waveguide is less than 0.5 dB with the MMF, as shown in Fig. 4(b). If the dimensions of the metal-slot width and the dielectric thickness are 12 μm, the MFD of the waveguide is about 9.5 μm and satisfactory coupling loss may be achievable with a SMF. The dependence of the propagation loss on the polarization is not noticeable.

To demonstrate the ability of the PCB-compatible metal-slotted hybrid optical waveguide to transmit optical data, we performed the transmission experiment of 2.5 Gbps optical signals, referring to the previous study [15, 16]. Figure 5(a) shows the assembled high-speed optical signal transmission experiment set-up with the 3 cm-long metal-slotted hybrid optical waveguide. The input and the output facets of the hybrid optical waveguide are coupled with the vertical cavity surface emitting laser (VCSEL) and the photodiode, respectively. The VCSEL with a 1.3 μm wavelength is installed in the optical transmitter (Tx) module that consists of a VCSEL driver IC, numerous electrical components, the SMA connector, the Tx test board, and the connector between board and module. An electrical signal from a pulse pattern generator (PPG) is transmitted to the VCSEL on the (Tx) module. A modulated optical signal from the VCSEL is transmitted to the input facet of the hybrid optical waveguide via a direct end-fire coupling. Subsequently, the wave propagates along the waveguide, and then the beam reaches a photodiode in the optical receiver (Rx) module. The electrical signal from the PD in the Rx module is magnified by the receiver ICs such as a trans-impedance amplifier (TIA) and limiting amplifier. Finally, the electrical data are analyzed by using digital communication analyzer (DCA).

#164850 - $15.00 USD Received 16 Mar 2012; revised 9 Apr 2012; accepted 11 Apr 2012; published 20 Apr 2012

Figure 5(b) exhibits the measured eye diagram of the 2.5 Gbps optical signal transmitted via 3 cm-long metal-slotted hybrid optical waveguide. A 2.5 Gbps non-return-to-zero pseudorandom bit sequence (2^{31}-1) of the optical signals was generated at the VCSEL in the Tx module. The eye diagram for one optimized waveguide channel was clearly open at room temperature. The measured eye diagram is nearly identical with the eye pattern of the original back-to-back signal (the inset of Fig. 5(b)). The root mean square and the peak-to-peak timing jitter of the transmitted signal are 18.7 ps and 135 ps, respectively. The measured jitters are less than 10 ps from the original signals, which mean that the pulse broadening by the waveguide dispersion is negligible, as we expected. The bit error rate (BER) was estimated to be 10^{-10} under the best condition. From the clearly opened eye diagram, we confirmed that the proposed metal-slotted hybrid optical waveguide has an ability to transmit high-speed digital signals up to 2.5 Gbps without any pulse distortion. The lateral distance between the channels is large as 500 μm, which is enough to suppress the mode coupling between the channels. Therefore, the crosstalk is not measured during the optical data transmission experiment.

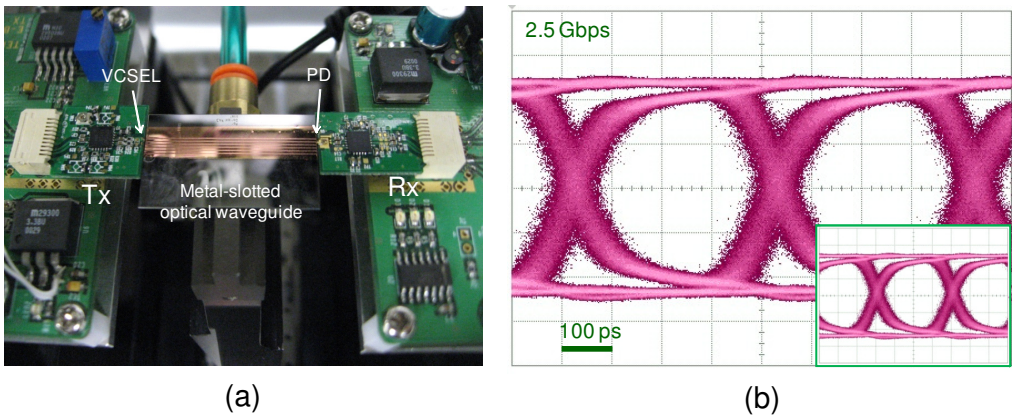

Fig. 5. Assembled optical signal transmission experiment set-up. (a) The input and the output facets of the fabricated metal-slotted hybrid optical waveguide are coupled with the VCSEL and the photodiode, respectively. (b) Measured optical eye diagram for 2.5 Gbps modulated optical signal.

For realization of an EOPCB system using the proposed metal-slotted hybrid optical waveguide, promising solutions for the optical coupling between the hybrid optical waveguide that is embedded in PCB and the optoelectronic devices such as VCSELs and PDs. This requirement demands 90° beam redirection in EOPCB systems. Fortunately, there are numerous optical coupling schemes that uses a surface-mounted 45° mirror or in/out coupling elements [17–19]. With the aid of these efficient coupling methods, innovative EOPCB systems using metal-slotted hybrid optical waveguide can be exploited further.

4. Conclusion

To provide an alternative solution for realization of electrical optical circuit board (EOCB) and electro-optical printed circuit board (EOPCB) systems, PCB-compatible metal-slotted hybrid optical waveguide was proposed and its optical characteristics are investigated at a wavelength of 1.31 μm. The metal film with wide slot is embedded in a dielectric layer and the both sides of top and bottom of the dielectric are covered with the metal film of infinite width. By using Cu electric circuit structure in the conventional PCB layer, the proposed hybrid optical waveguide provides high compatibility to PCB structures. The propagation loss of the waveguide was 1.5 dB/cm at the telecom wavelength of 1.31 μm. 2.5 Gbps data transmission without any pulse distortion was successfully accomplished with 3 cm-long metal-slotted hybrid optical waveguide. Based on these experimental results, we concluded that the proposed hybrid optical waveguide can be exploited further for development of next-generation EOCB and EOPCB systems.

#164850 - $15.00 USD Received 16 Mar 2012; revised 9 Apr 2012; accepted 11 Apr 2012; published 20 Apr 2012

Acknowledgments

This work has been supported by the S/W Computing R&D program of MKE/KEIT (10035360-2010-01, TAXEL: Visio-haptic Display and Rendering Engine).

#164850 - $15.00 USD Received 16 Mar 2012; revised 9 Apr 2012; accepted 11 Apr 2012; published 20 Apr 2012